

Experimental Investigation on Bed Shear Stress Distribution in a 180 Degree Sharp Bend by using Depth-Averaged Method

M. Vaghefi, M. Akbari, A. R. Fiouz

Department of Civil Engineering, Persian Gulf University, Bushehr, Iran.

Corresponding Author Email: vaghefi@pgu.ac.ir

Abstract : *Because of the great importance of shear stress parameter in river sediment transport mechanisms, different methods for calculating them are presented. This paper has used Depth-Averaged Method to study and analyse shear stress distribution near the bed in a 180 degree sharp bend. The results suggested that the maximum dimensionless shear stress near the bed occurs at the beginning of the bend, near the inner wall and in the 40 degree cross section.*

Keywords

180 Degree Bend, Sharp Bend, Bed Shear Stress, Depth-Averaged Method, Vectrino.

I. Introduction

Water flowing in an open channel exerts a longitudinal shear force on the wetted perimeter of the flow cross section, which tends to erode the channel walls. The boundary shear stress is one of the most important parameters in open channel flow but at the same time also one of the most difficult to analyse from a purely theoretical point of view. The influence of secondary flow, cross sectional shape, and non-uniform roughness distribution around the wetted perimeter all combine to make the prediction of the boundary shear stress distribution very difficult even for simple cases [i].

Bed shear stress plays a key role in the mechanism of transportation of sediment of the rivers; therefore, many researchers have conducted studies on how to measure bed shear stress in river bends. Based on the studies carried out by Ze'ev B. Begin in 1986 [ii], and those by Yen & Shin in 1995 [iii], when $R/B > 3.5$ shear stress distribution at the entrance of the bend is almost constant, and maximum shear stress occurs at the end of the bend, near the outer wall. When $R/B < 3.5$, shear stress occurs both at the end of the bend, near the outer wall, and at the beginning of the bend, near the inner wall. Blanckaert & Graf in 2001, conducted an experimental study on the mean and turbulent flow pattern in a 120 degree bend. They also studied Reynolds normal and shear stress [iv]. Booij in 2003, adopted the LES method in order to simulate flow pattern in a 180 degree mild bend. He stated that the turbulence models such as $k-\epsilon$ would not simulate the secondary flow near the outer wall. He also measured Reynolds stresses in that flume [v]. Yang in 2005, studied the interaction between boundary shear stress, and the distribution of velocity and secondary flows in open channels. He also found the equations governing Reynolds shear stress distribution, and boundary shear stress [vi]. Ruther and Olsen in 2005, simulated the secondary flow and transportation of

sediment in a 90 degree narrow flume by using the $k-\epsilon$ turbulence model. The results of their simulation indicate that the direction of sediment transport depends on the direction of the shear stress near the bed [vii]. Barbhuiya and Talukdar in 2010, carried out an experimental study of 3D flow pattern and scour in a 90 degree bend. They measured time averaged velocity components, turbulence intensity, and Reynolds shear stress [viii]. Naji et al. in 2010, did experimental and numerical studies of flow pattern in a 90 degree bend and concluded that stream lines at a depth close to the bed orient to inner wall and at depths near the surface of water orient to outer wall. She also calculated the strength of secondary flow and bed shear stress [ix]. In 2012, Uddin and Rahman conducted an experimental study of 3D flow pattern and erosion by using ADCP velocimeter in the bend of the Jamuna River. They measured 3D velocity of the flow and shear stress near the bed of the river, and presented a model in order to predict erosion in the bend, based on the processes of the flow [x]. In 2014, Liaghat et al. carried out a numerical study of the hydraulic of the flow in a U-shaped flume with changing width by using SSIIM software. They studied 3D velocity components of the flow, shear stress, and the strength of the secondary and spiral flows [xi].

Since most of the studies on bed shear stress have been carried out by using Reynolds Shear Stress method, in this paper, Depth-Averaged method has been used to calculate bed shear stress in a 180 degree sharp bend.

II. Material and Methodology

■ Experimental Model Introduction

■ Laboratory Flume

A 1 meter wide, and 0.7 meter deep bend flume with a 180 degree central bend, which has glass walls and steel frames, was designed and built for this experiment, in the laboratory of advanced hydraulic structures in Persian Gulf University in Iran. A picture of the flume located in the laboratory, and the schematic plan, along with its geometric specifications are presented in Figures 1, and 2 respectively. As is seen, the flume has a 180 degree central bend, with an upstream 6.5 meter straight reach, and a downstream 5 meter straight reach. As is observed in the figure, the 180 degree bend with a 2.5 meter external radius connects the two reaches. Since the flume is 1 meter wide, according to Rodi classification, it can be considered a sharp bend flume. ($R/B = 2 < 3$) [xii]. Reservoirs are placed under the flume in order to provide a capacity of 30 m³ of water. The pump has a discharge of 90 lit/s which is constant during the experiment. The depth of the water is also constant, equal to 20 cm at the entrance of the

bend, which is adjusted for the sake of the experiment by using the butterfly gate at the end of the downstream reach.



Figure (1): a view of the 180 degree sharp bend multipurpose flume located in the laboratory of advanced hydraulic structures in Persian Gulf University.

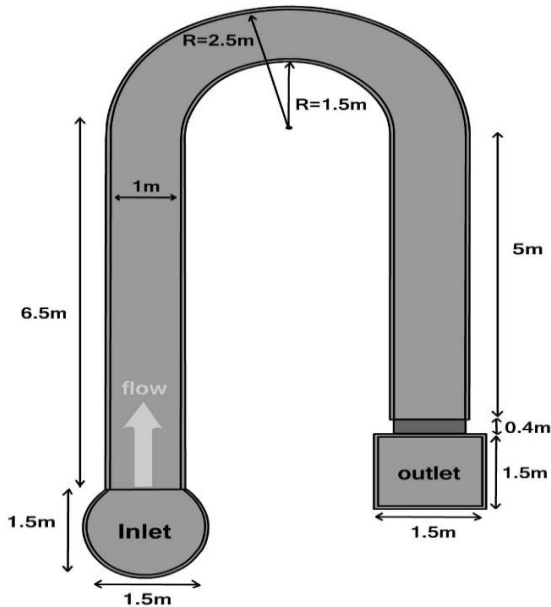


Figure (2): The schematic plan and specifications of the flume.

▪ The Vectrino (3D Water Velocimeter) and its Softwares

The Vectrino is a high-resolution acoustic velocimeter used to measure 3D velocity of water. Different probes of this device are provided in Figure 3 [xiii]. The side looking device is used to measure the velocity of the flow near the walls of the flume and the water surface, and the down looking device is used in other situations. The velocity range is from ± 0.01 to ± 7 m/s, and is adjustable for the user with $\pm 5\%$ measured accuracy (± 1 mm/s). [xiv] The experiments will be carried out at a 25 Hz frequency in 1 minute. Therefore, the device can record up to 1500 data of the flow velocity per second in three directions. In Figure 4, the position of the velocimeter in a 180 degree bend, and the software used to save the data are shown.



Figure (3): Two different probes of the Vectrino. On the right, the receiving beams on down looking mode, and on the left, the receiving beams on side looking mode [xiii].

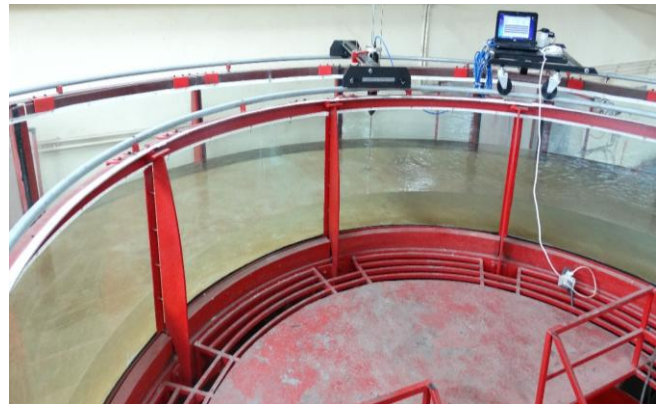


Figure (4): Measuring the 3D velocity of the flow in a 180 degree bend by using the Vectrino and its softwares.

▪ Planning and Conducting the Experiments

The data related to 3D velocity components of the flow were recorded in a maximum distance of 5 mm from the bed in order to determine the exact shear stress near the bed of the flume. In order to measure the velocity of the flow near the bed, 23 sections from the beginning to the end of the bend, each of which having 12 cross sections, are used.

▪ Calculation of Bed Shear Stress

Various methods have been offered to date to determine shear stress parameter because of its high importance in river engineering field. Each of the methods can be used to measure bed shear stress through flow field, considering the conditions governing the phenomenon. Since vertical velocity component is smaller than the other two components, the Depth-Averaged method has been utilized in this paper in order to measure bed shear stress in a 180 degree sharp bend. This method measures bed shear stress along x direction (τ_x), y direction (τ_y) and the resultant bed shear stress (τ_b) through the following relations [xv]:

$$\tau_{bx} = C_f \cdot \rho \cdot \bar{u} (\bar{u}^2 + \bar{v}^2) \quad (1)$$

$$\tau_{by} = C_f \cdot \rho \cdot \bar{v} (\bar{u}^2 + \bar{v}^2) \quad (2)$$

$$\tau_b = C_f \cdot \rho \cdot (\bar{u}^2 + \bar{v}^2) \quad (3)$$

$$C_f = \frac{n^2 g}{y^3}$$

(4)

$$n = \frac{d_{50} \left(\frac{1}{6}\right)}{21.1} \quad (5)$$

Where,

τ_x , τ_y and τ_b represent shear stress along the length of the channel, the width of the channel, and the resultant shear stress respectively;

\bar{u} , \bar{v} represent measured velocities in depth along x, and y;

n, manning coefficient;

y, flow depth;

And g, acceleration of gravity.

III. Results and Tables

For analysis of shear stresses near the bed, shear stress in different locations in the bend has been calculated through Depth-Averaged method, and it has become dimensionless by upstream average shear stress (τ_0).

In Figures 5 and 6, the dimensionless shear stress contours and also its amounts near the bed in a 180 degree sharp bend is shown. As it is observed, maximum shear stress occurs at the beginning of the bend, near the inner wall, because of longitudinal pressure gradient present at the beginning of the sharp bend. From the beginning to the middle of the bend, the highest amount of shear stress occurs from the inner wall to the middle of the channel. But after the first half of the bend, shear stress decreases by almost 50%. From 90 degree cross section to the bend exit, the maximum dimensionless shear stress occurs near the outer wall. It can be concluded that if the bed of the channel is a live bed, because the shear stress at the beginning of the bend is up to several times the amount of that in an upstream straight reach, there will be scour and sediment launching towards the downstream of the bend.

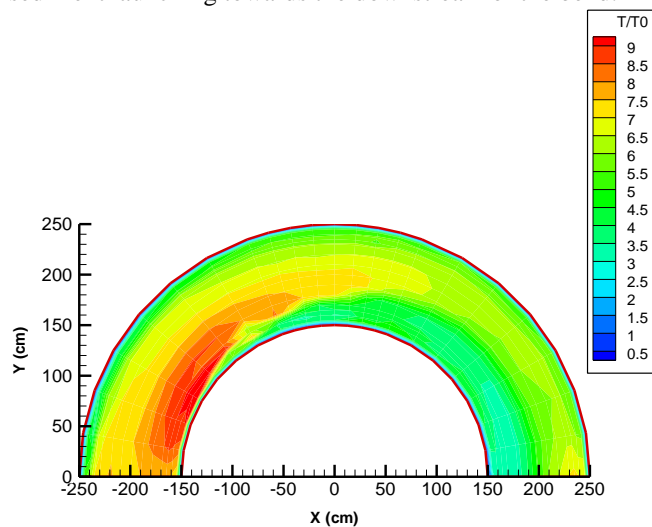


Figure (5): shear stress contours which have become dimensionless by upstream averaged shear stress in the 180 degree sharp bend by using Depth-Averaged method.

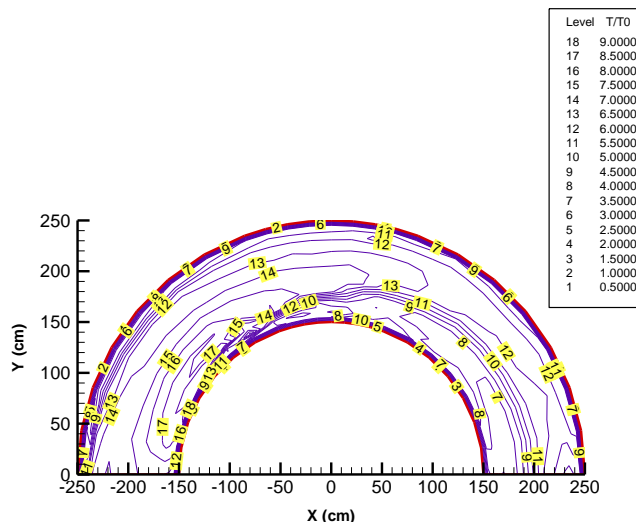


Figure (6): shear stress contour values which have become dimensionless by upstream averaged shear stress close to the 180 degree sharp bend through Depth-Averaged method.

In order to be investigated, maximum values of shear stresses throughout a bend have been calculated and become dimensionless by τ_0 . Figure 7 presents the maximum values for shear stress near the bed in different sections of a 180 degree sharp bend. As is seen in the figure, the highest amount of dimensionless shear stress occurs in the 40 degree cross section, and it is about 9.25 times the amount of the upstream average shear stress. High velocities at the beginning of the bend lead to a sharp increase in stress in the beginning sections of the sharp bend. But in the second half of the bend, dimensionless shear stress decreases to the point that the least amount of dimensionless stress is observed in the 160 degree section. Before the flow passes the bend completely, in the 180 degree cross section, there is an increase in dimensionless shear stress again.

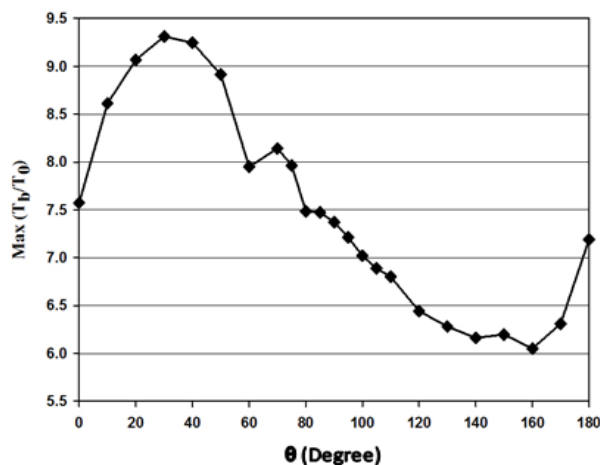


Figure (7): Maximum values for dimensionless shear stress in different sections of a 180 degree sharp bend.

Figure 8 presents the variations in the maximum dimensionless shear stress throughout the bend. As it is observed, from the beginning to the top of the bend,

maximum shear stress occurs near the inner wall, but thereafter, it is oriented towards the middle of the channel, and finally occurs near the outer wall at the end of the bend.

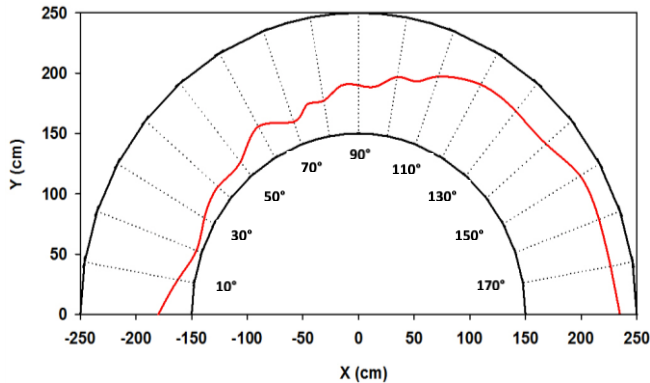


Figure (8): Maximum dimensionless shear stress variations throughout the bend.

A diagram of the variations in the dimensionless shear stress at different distances from the outer bank (5%, 50% and 95% of the width from the outer wall) is presented in Figure 9. It can be observed in the figure that the maximum dimensionless shear stress occurs at a distance of 5% of the width from the outer wall, at the bend exit in the 180 degree cross section. But in the middle of the channel, the maximum dimensionless shear stress occurs in the first half of the bend, especially at the beginning. The most variations of dimensionless shear stress occur near the inner wall; therefore, the maximum dimensionless shear stress occurs at the beginning of the bend, and the minimum dimensionless shear stress at the end of it.

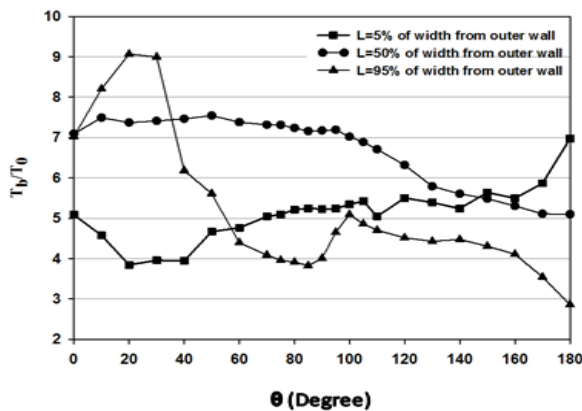


Figure (9): dimensionless shear stress variations at different distances from the outer bank.

IV. Conclusion

This paper uses the Depth-Averaged method to study the amount of dimensionless shear stress in a 180 degree bend, and the results are presented as follows:

- 1-The maximum dimensionless shear stress occurs at the beginning of the bend, near the inner wall.
- 2-The maximum dimensionless shear stress in the second half of the bend occurs near the outer wall.
- 3-The maximum dimensionless shear stress occurs in the 40 degree cross section, and the minimum in the 160 degree cross section.
- 4-The most variations of dimensionless shear stress were observed near the inner wall.

References

- i. Ansari, K. (2011). *Boundary shear stress distribution and flow structures in trapezoidal channels* (Doctoral dissertation, University of Nottingham).
- ii. Begin, Z. E. B. (1986). *Curvature ratio and rate of river bend migration-update*. *Journal of Hydraulic Engineering*, Vol. 112, No. 10, pp. 904-908.
- iii. Yen, C. L. and Ho, S. Y. (1990). *Bed evolution in channel bends*. *Journal of Hydraulic Engineering*, Vol. 116, No. 4, pp. 544-562.
- iv. Blanckaert, K. and Graf, W. H., (2001). *Mean flow and turbulence in open-channel bend*. *Journal of Hydraulic Engineering*, Vol. 127, No. 10, pp. 835-847.
- v. Booij, R. (2003). *Measurements and large eddy simulations of the flows in some curved flumes*. *Journal of Turbulence*, Vol. 4, No. 1, pp. 8.
- vi. Yang, S. Q. (2005). *Interactions of boundary shear stress, secondary currents and velocity*. *Fluid dynamics research*, Vol. 36, No. 3, pp. 121-136.
- vii. Ruther, N. and Olsen, B. (2005). *Three dimensional modeling of sediment transport in a narrow 90 channel bend*. *Journal of Hydraulic Engineering*, Vol. 131, No. 10, pp. 917-920.
- viii. Barbhuiya, A. K. and Talukdar, S. (2010). *Scour and three dimensional turbulent flow fields measured by ADV at a 90 degree horizontal forced bend in a rectangular channel*. *Flow Measurement and Instrumentation*, Vol. 21, No. 3, pp. 312-321.
- ix. Naji Abhari, M., Ghodsian, M., Vaghefi M. and Panahpur, N. (2010). *Experimental and numerical simulation of flow in a 90 degree bend*. *Flow Measurement and Instrumentation*, Vol. 21, No. 3, pp. 292-298.
- x. Uddin, M. N. and Rahman, M. M. (2012). *Flow and erosion at a bend in the braided Jamuna River*. *International Journal of Sediment Research*, Vol. 27, No. 4, pp. 498-509.
- xi. Liaghat, A., Mohammadi, K. and Rahmanshahi, M. (2014). *3D Investigation of Flow Hydraulic in U Shape Meander Bends with Constant, Decreasing and Increasing Width*. *Journal of river engineering*, Vol. 2, No. 3, pp. 12-23.
- xii. Leschziner, M. A. and Rodi, W. (1979). *Calculation of strongly curved open channel flow*. *Journal of the Hydraulics Division*, Vol. 105, No. 10, pp. 1297-1314.
- xiii. Nortek Vectrino Velocimeter User Guide (2004). Nortek USA.
- xiv. Rusello, P. J. (2009). *A Practical Primer for Pulse Coherent Instruments*. Nortek USA.
- xv. Tingsanchali, T. and Maheswaran, S. (1990). *2-D depth-averaged flow computation near groyne*. *Journal of Hydraulic Engineering*, Vol. 116, No. 1, pp. 71-86.